DOI: 10.1002/ejoc.200500499

pH-Dependence in the Hydrolytic Action of the Human Fragile Histidine Triad

Kaisheng Huang,[a] Abolfazl Arabshahi,[a] and Perry A. Frey*[a]

Dedicated to Professor Wojciech Stec on the occasion of his 65th birthday

Keywords: Enzymes / Hydrolases / Enzyme catalysis / Hydrolysis / Kinetics

The human fragile histidine triad protein (Fhit) is a member of the HIT family of enzymes, which catalyze hydrolysis or nucleotidyltransfer reactions of dinucleoside polyphoshates. Fhit catalyzes the magnesium ion-dependent hydrolysis of P^1–5′-*O*-adenosine-P^3–5′-*O*-adenosine triphosphate (Ap_3A) to adenosine-5′-*O*-phosphate (AMP) and the magnesium complex of adenosine-5′-*O*-diphosphate (ADP) by a double displacement mechanism, with the formation of an adenylyl enzyme as an intermediate. Fhit also catalyzes the hydrolysis of adenosine-5′-phosphoimidazolide (AMP-Im) and adenosine-5′-phospho-*N*-methylimidazolide (AMP-*N*-MeIm). The pH-dependence of these reactions is reported herein, in which the principal conclusions are as follows: The action of wild-type Fhit on $MgAp_3A$ is diffusion-limited and on AMP-Im and AMP-*N*-MeIm largely diffusion-limited and largely pH-independent. The actions of specifically mutated H96G-Fhit on AM-Im, and on AMP-*N*-MeIm, are not diffusion-limited and are pH-dependent. The actions of mutated forms of Fhit, H94G-Fhit, H98G-Fhit, and H94/98G-Fhit, are also not diffusion-limited and are pH-dependent. Log plots of kinetic parameters against pH show breaks that indicate a group on the enzyme must be protonated for maximal activity. Extensive analysis shows that the imidazole ring of His94 is not essential for the hydrolysis of $MgAp_3A$ or AMP-imidizolides, and the imidazole ring of His98 engages in binding the substrates. In the hydrolysis of AMP-Im, Fhit and its His94, His96, and His98 variants bind the monoanionic form of AMP-Im, and the proton required for formation of imidazole in the hydrolytic process originates with an acid/base group of the enzyme. Fhit and several variants also catalyze the hydrolysis of *p*-nitrophenyl-AMP.

Introduction

The fragile histidine triad (Fhit) protein is encoded by the human gene *FHIT* and, presumably by way of a signaling activity, functions as a tumor suppressor.[1] Tumor cells and cells in tumor-derived lines display deletions or aberrant transcripts of *FHIT*.[2–7] Fhit is a dimer of identical 20 kDa subunits, each of which contains a triad of histidine residues, His^{94}-Val^{95}-His^{96}-Val^{97}-His^{98} that is conserved as HxHxHxx in other species, with the residues "x" being hydrophobic. The structures of Fhit and other histidine triad (HIT) proteins reveal an overall chain fold for the dimer that is similar to the fold of a single subunit in galactose-1-P uridylyltransferase (GalT) from *E. coli*.[8–13] GalT catalyzes the reaction of galactose-1-phosphate (Gal-1-P) with uridine-5′-diphosphate glucose (UDPGlc) to form uridine-5′-diphosphate galactose UDPGal and glucose-1-phosphate (Glc-1-P) by a double displacement mechanism [Equation (1) and Equation (2)].

$$\text{UDPGlc} + \textbf{E}\text{-His}^{166} \rightleftharpoons \textbf{E}\text{-His}^{166}\text{\_UMP} + \text{Glc–1–P} \quad (1)$$

$$\textbf{E}\text{-His}^{166}\text{-UMP} + \text{Gal-1-P} \rightleftharpoons \textbf{E}\text{-His}^{166} + \text{UDPGal} \quad (2)$$

The nucleophilic catalyst His^{166} is the central residue in a conserved triad of two histidines and one glutamine, His^{164}-Pro^{165}-His^{166}-Gly^{167}-Glu^{168}.[14–24]

As an enzyme, Fhit catalyzes the Mg^{2+}-dependent hydrolysis of P^1–5′-*O*-adenosine-P^3–5′-*O*-adenosine triphosphate (Ap_3A) to adenosine-5′-*O*-phosphate (AMP) and the Mg^{2+} complex of adenosine-5′-*O*-diphosphate (ADP) by cleavage of the P_α–O bond and not the P_β–O bond.[25–27] The hydrolysis of a P-chiral analog of Ap_3A in $H_2{}^{18}O$ proceeds with overall retention of configuration at P, consistent with a double displacement mechanism of hydrolysis, as in the reaction of GalT.[28] The apparent similarities of the active site triads in Fhit and GalT, and the similar chain folds of the two enzymes inspired the proposition of similar mechanisms for the two reactions. According to this hypothesis, the action of Fhit also follows a double displacement mechanism, in which the ultimate adenylyl group acceptor is water [Equation (3) and Equation (4)].

[a] Department of Biochemistry, University of Wisconsin – Madison,
1710 University Avenue, Madison, Wisconsin 53726, USA
E-mail: frey@biochem.wisc.edu

$$Ap_3A + E^{Fhit}\text{-}His^{96} \rightleftharpoons E^{Fhit}\text{-}His^{96}\text{-}AMP + ADP \quad (3)$$

$$E^{Fhit}\text{-}His^{96}\text{-}AMP + H_2O \rightleftharpoons E^{Fhit}\text{-}His^{96} + AMP \quad (4)$$

Evidence supporting this mechanism includes the observation of a trace of protein-bound ^{32}P when Fhit is mixed with the poor substrate [α-^{32}P]ATP (adenosine-5′-*O*-triphosphate), the observation of 11% adenylylation of Fhit by [8,8′-^{3}H]Ap_3A based on tritium incorporation, the observation of Fhit-catalyzed exchange of [^{3}H]ADP into Ap_3A, and the observation of overall retention of configuration at phosphorus consistent with double inversion in two steps.[27–29]

The crystal structures of GalT and Fhit strongly suggest that nucleotidyl group transfer catalyzed by His^{166} in GalT and His^{96} in Fhit proceeds with participation of the main-chain carbonyl group of the conserved histidine two residues upstream, His^{164} in GalT and His^{94} in Fhit. In each structure, the upstream histidine main-chain carbonyl group is in position to accept a hydrogen bond from the imidazole ring of the nucleophilic histidine in the covalent nucleotidyl enzyme intermediate, as illustrated in Figure 1. Acting in this capacity, the main-chain carbonyl group could maintain the protonated, imidazolium moiety in the covalent intermediate. This should potentiate the nucleotidyl transfer activity of the intermediate because the neutral species would be chemically far less reactive. A nucleoside-5′-phosphoimidazolide is not basic enough to exist in the imidazolium form at physiological pH; for example the value of pK_a for the imidazolium group of UMPIm is 5.68.[30]

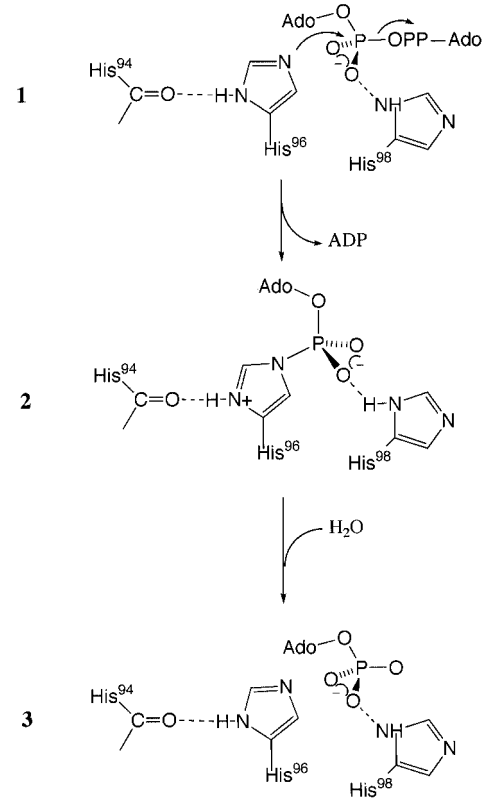

Figure 1. A mechanism for Fhit-catalyzed hydrolysis of $MgAp_3A$.

The mechanism in Figure 1 cannot be tested by X-ray crystallography until sufficiently high resolution is attained to obtain images of protons in the GalT-His^{166}-UMP intermediate. We have undertaken to study this mechanism kinetically in chemically rescued reactions of the specifically mutated Fhit, Fhit-H96G. We here report our studies of pH-dependence in the actions of H96G-Fhit, wild-type Fhit, and other variants of Fhit on Ap_3A, adenosine-5′-phosphoimidazolide (AMP-Im) and adenosine-5-phospho-*N*-methylimidazolide (AMP-*N*-MeIm).

Results

Catalytic Properties of H96G-Fhit

The phosporamidase activity of H96G-Fhit toward AMP-Im corresponds to the chemical rescue of the variant.[29] The complex of H96G-Fhit with AMP-Im should be analogous to the covalent intermediate $\mathbf{E}^{Fhit}$-His^{96}–AMP in Equation 3 and Equation 4 (**2** in Figure 1), in that the imidazole ring of AMP-Im should occupy the vacated subsite for the imidazole ring of His^{96}, and the AMP moiety should occupy the same binding site as in the covalent intermediate. Then H96G-Fhit catalyzes the hydrolysis of AMP-Im, as in the hydrolysis of $\mathbf{E}^{Fhit}$-His^{96}–AMP in Equation (4) (**2** to **3** in Figure 1). The kinetic parameters k_{cat} and k_{cat}/K_m for hydrolysis of AMP-Im by the variant are about 1/50th those for the hydrolysis of Ap_3A by wild-type Fhit.[29] The parameters for the action of wild-type and H96G-Fhit are listed in Table 1, together with values for other variants of Fhit.

H96G-Fhit also catalyzes the hydrolysis of AMP-*N*-MeIm at a maximum rate that is comparable to the value for the hydrolysis of AMP-Im.[29] The value of K_m in the

Table 1. Kinetic parameters for hydrolysis of substrates by Fhit and selected variants.[a]

Enzyme	Ap_3A k_{cat}[a]	Ap_3A k_{cat}/K_m	Substrate AMP-Im k_{cat}	AMP-Im k_{cat}/K_m	AMP-*N*-MeIm k_{cat}	AMP-*N*-MeIm k_{cat}/K_m
wt-Fhit[b]	3.5 ±.1	1160 ± 72	4.4 ± .1	642 ± 16	4.2 ± .1	717 ± 25
H96G[b]	ND	ND	0.91 ± .03	35 ± 1	0.62 ± .06	1.9 ± .01
H94G	0.48 ± .01	1083 ± 48	0.57 ± .02	737 ± 33	–	–
H98G	0.07 ± .01	0.47 ± .02	0.51 ± .01	11.3 ± .1	0.24 ± .02	31 ± 1
H94/98G	0.05 ± .01	0.27 ± .01	0.06 ± .01	2.1 ± .1	0.07 ± .03	9.7 ± .6

[a] Kinetic parameters are k_{cat} [s^{-1}] and k_{cat}/K_m [mM^{-1} s^{-1}]. [b] Previously reported in ref.[29]

hydrolysis of AMP-*N*-MeIm is significantly higher than in the hydrolysis of AMP-Im, presumably because of the greater steric requirements of the *N*-methylimidazole group relative to imidazole. The equivalent maximum velocities for the two substrates suggest that the rate-limiting step is the same for AMP-*N*-MeIm and AMP-Im within the Michaelis complexes.

pH-Dependence of Hydrolysis by H96G-Fhit

To address the question of the protonation state of the imidazole moiety in the nucleotidyl intermediate $\mathbf{E}^{Fhit}$-His^{96}–AMP in wild-type Fhit, we studied the pH-dependence for the action of Fhit-H96G on AMP-imidazolides. The pH-rate profiles for the hydrolysis of AMP-Im in Figure 2 show that both k_{cat} and k_{cat}/K_m are pH-dependent, with breaks in plots of log k_{cat} and log k_{cat}/K_m against pH, with high activity at pHs below 7 and much lower activity at high pHs. The profiles are compatible with the requirement that a single ionizing group in its conjugate acid form potentiates optimal enzymatic activity. The values of pK_a for the principal ionizations controlling the rate are 7.06 for k_{cat} and 6.87 for k_{cat}/K_m. The value for k_{cat} refers to an ionization of an enzyme-substrate complex, and that for k_{cat}/K_m refers to an ionization of either the free enzyme or the free substrate. The ionizations governing the pH-rate profiles cannot be assigned to AMP-Im (Scheme 1) because the value of pK_a for the phosphoimidazolide is 5.6 (see Experimental Section). Therefore, the pK_a values in Figure 1**A** and **B** must correspond to ionizations of the complex H96G-Fhit·AMP-Im and free H96G-Fhit, respectively. Moreover, the values of K_m for AMP-Im are essentially pH-independent (data not shown), so that the enzyme must be binding the anion of AMP-Im shown on the right side of Scheme 1.

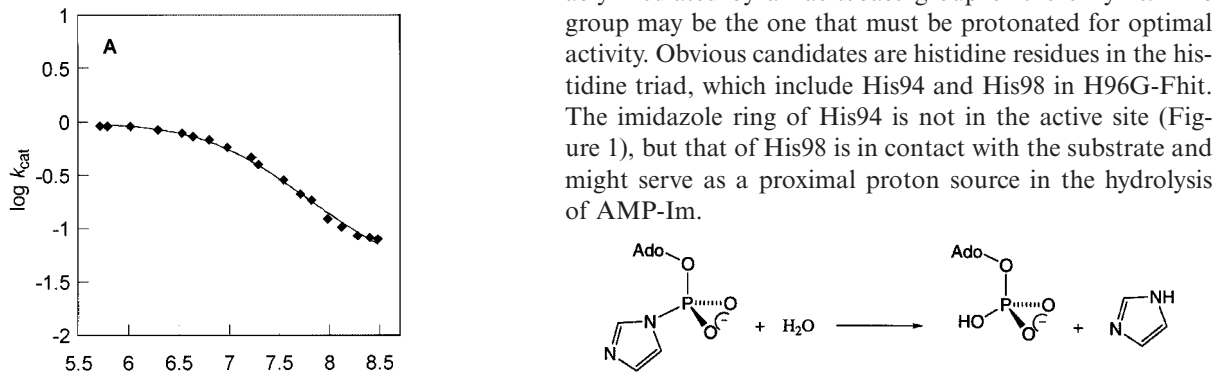

Figure 2. pH-Rate profiles for hydrolysis of AMP-Im by H96G-Fhit. Values of k_{cat} and K_m were determined in the pH range 5.5–8.5 at 26.5 °C as described in the Experimental Section. Panel **A** depicts a plot of log k_{cat} against pH. The solid line is calculated from the fit of data points to Equation (6), resulting in a value of pK_a = 7.06 ± 0.03. Panel **B** depicts a plot of log k_{cat}/K_m against pH. The fit of data points to Equation (6) yields a value of 6.87 ± 0.03 for pK_a, and the solid line is calculated for this value.

Scheme 1.

In the hydrolysis of AMP-Im, the imidazole ring must acquire a proton to form free imidazole (Scheme 2). While this proton ultimately arises from the water that is cleaved in the overall hydrolytic process, proton transfer is presumably mediated by an acid/base group of the enzyme. This group may be the one that must be protonated for optimal activity. Obvious candidates are histidine residues in the histidine triad, which include His94 and His98 in H96G-Fhit. The imidazole ring of His94 is not in the active site (Figure 1), but that of His98 is in contact with the substrate and might serve as a proximal proton source in the hydrolysis of AMP-Im.

Scheme 2.

If the phosphoimidazolide groups of AMP-Im and the covalent intermediate $\mathbf{E}^{Fhit}$-His^{96}-AMP react in their protonated states as in Figure 1, then the pH-rate profile for the H96G-Fhit-catalyzed hydrolysis of AMP-*N*-MeIm should differ from that for the hydrolysis of AMP-Im. This is because the imidazole ring in AMP-Im is not protonated in neutral solution (pK_a = 5.6) and the *N*-methyl group in AMP-*N*-MeIm maintains the quaternary nitrogen in the imidazole ring and therefore does not require a proton to react. Scheme 3 illustrates the hydrolysis of AMP-*N*-MeIm. In effect, the *N*-methyl group serves as a surrogate proton in the hydrolysis.

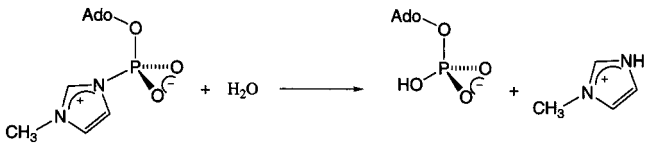

Scheme 3.

The pH-rate profiles in Figure 3**A** and **B** for the hydrolysis of AMP-*N*-MeIm are unlike those in Figure 2 for the reaction of AMP-Im. The profiles for k_{cat} and k_{cat}/K_m show two breaks, with identical values of 5.3 for the pK_a on the acid side and 7 on the alkaline side. The higher value of pK_a is likely to correspond to the same ionization as in the hydrolysis of AMP-Im. The lower pK_a must represent the ionization of a group on H96G-Fhit, in which the conjugate acid state is less active than the unprotonated state. The results show that the enzyme can be "overprotonated" for the hydrolysis of AMP-*N*-MeIm, presumably because of the charge type of AMP-*N*-MeIm as a zwitterion brought about by the *N*-methyl group.

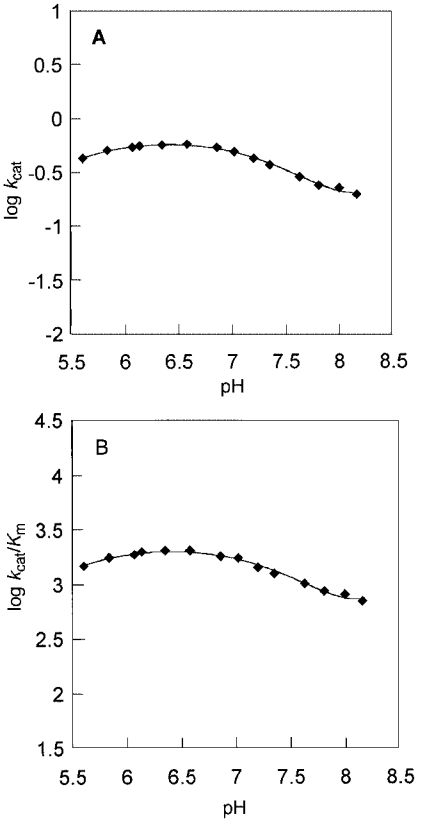

Figure 3. pH-Rate profiles for hydrolysis of AMP-*N*-MeIm by H96G-Fhit. Panel **A** is a plot of log k_{cat} against pH for rates measured at 26.5 °C as described in the Experimental Section. The solid line represents the fit of data points to Equation (8) with two values of pK_a, =5.35 ± 0.08 and 7.43 ± 0.03. Panel **B** is a plot of log k_{cat}/K_m against pH with the data fitted to Equation (7). The solid line is calculated based on 5.35 and 7.42 as the values of pK_a.

While H96G-Fhit alone does not catalyze the hydrolysis of $MgAp_3A$, it is chemically rescued by free imidazole and catalyzes the imidazole-dependent hydrolysis of $MgAp_3A$.[29] The pH-dependence of this reaction at 0.55 M imidazole is shown in Figure 4. In Panel **A**, the plot of log k_{cat} against pH shows increasing rate with increasing pH, a slope of +1, and a break corresponding to pK_a = 7.09: This is the value of pK_a for imidazole, and the rate-dependence on pH is assigned to the reaction of the enzyme–substrate complex with free imidazole, which must be in the form of its conjugate base to react in the chemical rescue. The plot of log k_{cat}/K_m against pH is more complex, bell-shaped, and shows two breaks corresponding to pK_a-values of 5.72 and 7.84. The $MgAp_3A$ does not undergo ionizations in this pH range, so that the transitions in Figure 4**B** must represent ionizations of the free enzyme (H96G-Fhit).

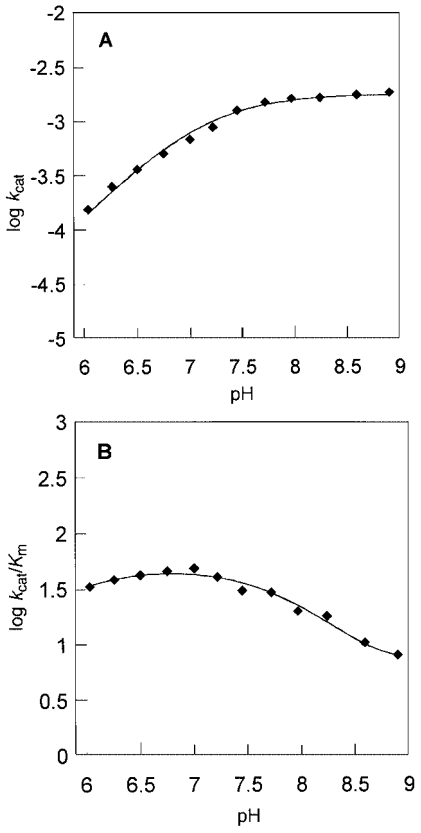

Figure 4. pH-Rate profiles for hydrolysis of Ap_3A in 0.55 M imidazole by H96G-Fhit. Panel **A** is a plot of log k_{cat} against pH at 26.5 °C in the pH range of 6.0–8.9. The data were fitted to Equation (5) and gave 7.09 ± 0.03 as the value of pK_a. The solid line is calculated for a pK_a value of 7.09. Panel **B** is a plot of log k_{cat}/K_m against pH, with the data points fitted to Equation (8). The two values of pK_a were 5.72± 0.18 and 7.84 ± 0.03, and the solid line is calculated for these values.

pH-Dependence of Wild-Type Fhit

Until recently, the best substrate for wild-type Fhit has been $MgAp_3A$. However, the wild-type enzyme also catalyzes the hydrolysis of AMP-Im and AMP-*N*-MeIm equally as well, the difference being that the magnesium requirement for action on Ap_3A is absent in the hydrolysis of AMP-imidazolates.[29] The similarities in the kinetic parameters for the three substrates extend to the pH-dependence, as shown in Figure 5. Two facts stand out in the pH-rate profiles. First, the bell-shaped profiles are shallow and do not approach slopes of +1 and –1 at low and high pHs. Second, the rate constants are remarkably similar for the three substrates. Both of these facts suggest that the rate-limiting process may be similar for these substrates, and that diffusion may be rate limiting.

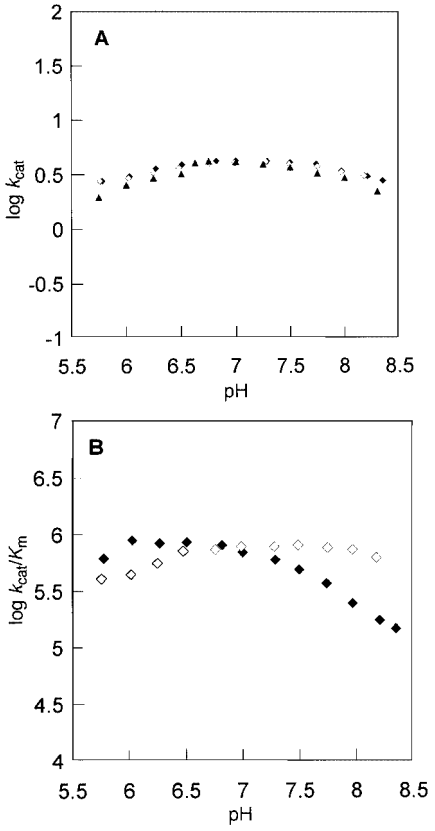

Figure 5. pH-rate profiles for hydrolysis of AMP-Im, AMP-*N*-MeIm, and Ap_3A by wild-type Fhit. Panel **A** shows plots of log k_{cat} against pH at 26.5 °C for the hydrolysis of AMP-Im (◊), AMP-*N*-MeIm (◊) and Ap_3A (▲). Panel **B** shows plots of log k_{cat}/K_m against pH for AMP-Im (◊) and AMP-*N*-MeIm (◊).

To assess the impact of diffusion on the rate constants, the effects of a viscogen on the rate constants were determined by the method of Brower and Kirsch,[34] with the results shown in Figure 6. In this method, the values of k_{cat}/K_m are determined in the presence and absence of a viscogen at several relative viscosities η_{rel} The parameters k_a^o and k_a are defined as the values of k_{cat}/K_m in the absence and presence of viscogens, respectively, and the ratios k_a^o/k_a are plotted against η_{rel} When diffusion is not rate limiting the slope of this plot is zero, and when diffusion is fully rate limiting the slope is +1. Figure 6 shows that the hydrolysis of $MgAp_3A$ by the action of wild-type Fhit is fully diffusion controlled, and the hydrolyses of AMP-Im or AMP-*N*-MeIm by action of H96G-Fhit are not at all limited by diffusion. The hydrolyses of AMP-Im or AMP-*N*-MeIm by wild-type Fhit are significantly diffusion limited as well. Therefore, diffusion limitation explains the shallow pH-dependencies and similarities in kinetic parameters in Figure 5. In contrast, diffusion does not limit rates in the actions of H96G-Fhit.

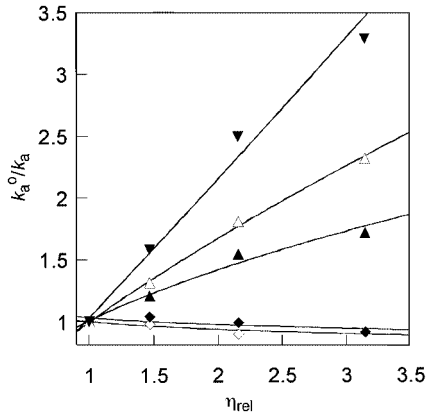

Figure 6. Viscosity effects on hydrolysis by H96G-Fhit and wild-type Fhit. Hydrolyses of AMP-Im, AMP-*N*-MeIm and Ap_3A were studied as a function of viscosity at 26.5 °C. The kinetic data are plotted as $k_a = k_{cat}/K_m$, $k_a^o = k_a$ ($\eta_{rel} = 1$). (◊) Hydrolysis of AMP-Im by H96G-Fhit, (◊) hydrolysis of AMP-*N*-MeIm by H96G-Fhit, (▲) hydrolysis of AMP-Im by wild-type Fhit, (Δ) hydrolysis of AMP-*N*-MeIm by wild-type Fhit, (▼) hydrolysis of Ap_3A by wild-type Fhit.

Importance of His94 and His98

The conserved histidine residues in the HIT enzymes are not equally important in catalysis, as shown by the kinetic parameters in Table 1. While His96 is essential in the hydrolysis of Ap_3A, His94 and His98 are less important. Mutation of His94 to glycine has very little effect on the values of k_{cat}/K_m in the hydrolysis of $MgAp_3A$ or AMP-Im, and values of k_{cat} are lower by seven- or eightfold in the action of H94G-Fhit relative to the wild-type enzyme. This may be attributed to the absence of the imidazole ring of His94 in the active site: the main chain carbonyl group of His94 is in hydrogen bonded contact with the imidazole ring of His96 (Figure 1).

Mutation of His98 brings about much greater decreases in kinetic parameters. Values of k_{cat} and k_{cat}/K_m for H98G-Fhit are 1/50th and 1/2500th the values for wild-type Fhit, respectively. H98G-Fhit is also much less active against AMP-Im and AMP-*N*-MeIm than the wild-type enzyme, 17 and 30-fold less active in terms of k_{cat}. A difference from the reaction of Ap_3A is that the values of k_{cat}/K_m are only 20- to 50-fold lower for H98G-Fhit. Double mutation of His94 and His98 further degrades the activity, especially against the AMP-phosphoramidates.

The pH-rate profiles for the actions of H94G-, H98G-, and the double variant H94/98G-Fhit with the three substrates are shown in Figure 7, panels **A** to **D**. The data for hydrolysis of AMP-Im by H94G- and H94.98G-Fhit in panels **A** and **B** are similar in displaying one break and a descending limb with increasing pH corresponding to pK_a-values of 6.8 to 7.9. In this respect, the profiles are analogous to those for H96G-Fhit in Figure 2. The data are consistent with a requirement for an acid/base group in its protonated form in the hydrolysis of AMP-Im. The results for H98G-Fhit are different (part **b** of panel **A**), and the log k_{cat} data are not fitted to an equation. The log k_{cat}/K_m plot is more analogous to the others, and this will be explained in a later section.

The pH-rate profiles for the hydrolysis of AMP-*N*-MeIm in panels **C** and **D** show little or no pH-dependence for k_{cat}

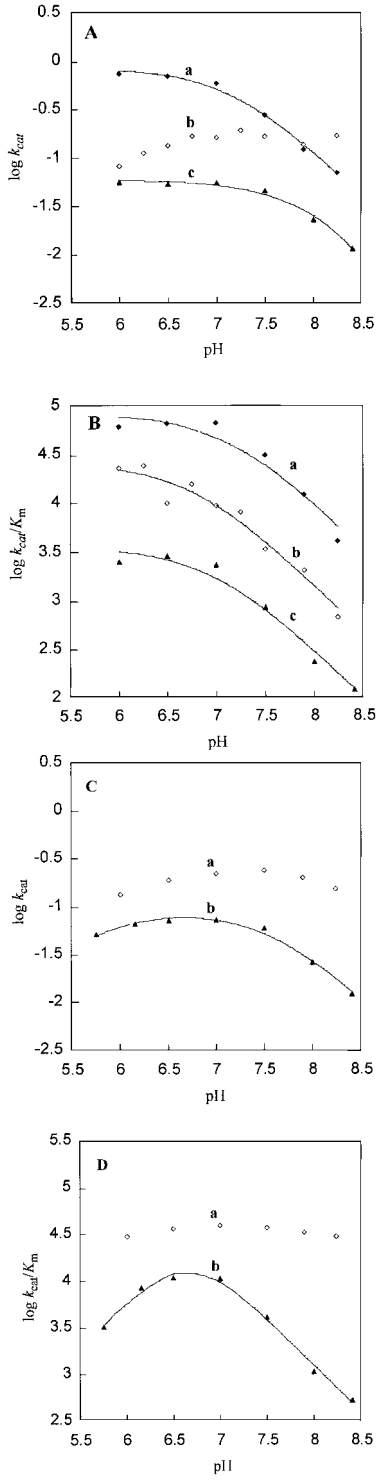

Figure 7. pH-Rate profiles for the hydrolysis of AMP-Im and AMP-*N*-MeIm by variants of Fhit. Panel **A**. Log k_{cat} is plotted against pH for the hydrolysis of AMP-Im by: **a**, H94G-Fhit, pK_a = 7.18 ± 0.06; **b**, H98G-Fhit; and **c**, H94/98G-Fhit, pK_a = 7.86 ± 0.05. Panel **B**. Log k_{cat}/K_m is plotted against pH for the hydrolysis of AMP-Im by: **a**, H94G-Fhit, pK_a = 7.11 ± 0.17; **b**, H98G-Fhit, pK_a = 6.75 ± 0.13; and **c**, H94/98G-Fhit, pK_a = 6.95 ± 0.13. Panel **C**. Log k_{cat} is plotted against pH for the hydrolysis of AMP-*N*-MeIm by: **a**, H98G-Fhit and **b**, H94/98G-Fhit, pK_a^1 = 5.61 ± 0.13 and pK_a^2 = 7.60 ± 0.06. Panel **D**. Log k_{cat}/K_m is plotted against pH for the hydrolysis of AMP-*N*-MeIm by: **a**, H98G-Fhit and **b**, H94/98G-Fhit, pK_a^1 = 5.69 ± 0.13 and pK_a^2 = 7.61 ± 0.13.

in the actions of H98G- and H94/98G-Fhit. They further confirm and extend the observation in Figure 3 that the ''overprotonation'' of the enzyme can inhibit the hydrolysis of AMP-*N*-MeIm. The pK_a-value for the enzymatic group that must be unprotonated is 5.69 (curve **b**, panel **D**).

Role of His98

Curves **b** in Figure 7**A** and **B** suggest a role for His98 in the hydrolysis of AMP-Im. This is clarified by considering the pH-dependencies of K_m in the hydrolysis of the two AMP-phosphoramidates. Values of log K_m are plotted against pH in Figure 8 for the hydrolysis of AMP-Im and AMP-*N*-MeIm catalyzed by H98G-Fhit. The data for AMP-Im describe a straight line with a slope of +1, whereas the values of log K_m for AMP-*N*-MeIm are independent of pH. Inasmuch as the mutation of His98 has little effect on k_{cat} (curve **b** in panel **A**), His98 must be required for binding AMP-Im, and it has no such effect on the binding of AMP-*N*-MeIm. The hydrolysis of AMP-Im requires proton transfer to the departing imidazole, and His98 is in position to transfer a proton to a leaving group. It is reasonable to assign this role to His98 in the hydrolysis of AMP-Im. The hydrolysis of AMP-*N*-MeIm does not require proton transfer, and its binding by H98G-Fhit is pH-independent.

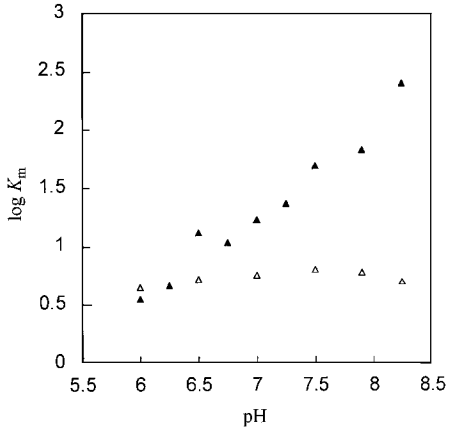

Figure 8. Plots of log K_m against pH for the hydrolysis of AMP-Im and AMP-*N*-MeIm by H98G-Fhit. The closed symbols are for the hydrolysis of AMP-Im and the open symbols for the hydrolysis of AMP-*N*-MeIm by H98G-Fhit.

p-Nitrophenyl-AMP as a Substrate

To further define the specificity of Fhit for leaving groups, we investigated *p*-nitrophenyl-AMP as a substrate. It is indeed a poor substrate for Fhit. The value of k_{cat} at pH 7.0 is 1.6 s^{-1} and the value of K_m is 2.5 mM. H96G-Fhit displays no detectable activity toward *p*-nitrophenyl-AMP. H94G- and H98G-Fhit are less active than wild-type Fhit, with respective values of 0.09 and 0.01 s^{-1} for k_{cat}, and 4.1 and 4.6 mM for K_m. Still, Fhit displays remarkable promiscuity in catalyzing the hydrolysis of AMP phosphodiesters,

phosphoramidates, and phosphoanhydrides. The AMP-phosphodiesterase activity of Fhit can be added to the many catalytic activities of HIT proteins.[35]

Discussion

Phosphoramidase Activities of Wild-Type Fhit

Because wild-type Fhit catalyzes the hydrolysis of Ap_3A, presumably by the double-displacement mechanism of Equation 3 and 4, and H96G-Fhit is completely inactive against Ap_3A, in agreement with the essential role of His 96 as the nucleophilic catalyst, it is of considerable interest that AMP-Im and AMP-*N*-MeIm are also substrates for wild-type Fhit. The kinetic parameters for wild-type Fhit show that AMP-Im and AMP-*N*-MeIm react nearly as efficiently as $MgAp_3A$. Clearly, the imidazole rings of AMP-Im and AMP-*N*-MeIm cannot be interacting with Fhit in the manner postulated above in hydrolysis by H96G-Fhit. The imidazole and *N*-methylimidazole rings of AMP-Im and AMP-*N*-MeIm are likely to react in the Fhit-catalyzed reactions simply as leaving groups in place of MgADP. Unlike the hydrolysis of $MgAp_3A$, Fhit-catalyzed hydrolysis of AMP-Im and AMP-*N*-MeIm is not dependent on Mg^{2+}. In the reaction of AMP-Im, His98 appears to mediate proton donation to the leaving imidazole. In this mechanism, AMP-Im (or AMP-*N*-MeIm) react with His96 to form the same covalent adenylyl-Fhit intermediate as in the reaction of $MgAp_3A$ in Equation (3) (**E**-His^{96}-AMP). This intermediate undergoes hydrolysis in the second step according to Equation (4).

Somewhat analogous to the plot of log K_m against pH in Figure 8, a similar plot for the hydrolysis of $MgAp_3A$ by H98G-Fhit displays a positive slope (data not shown). This is compatible with a role for His98 in binding $MgAp_3A$, as implied by the mechanism in Figure 1.

Phosphoramidase Activities of H96G-Fhit

Because of the absence of His96, H96G-Fhit cannot catalyze the hydrolysis of AMP-Im or AMP-*N*-MeIm by the same mechanism as Fhit. It must react with AMP-Im and AMP-*N*-MeIm in the manner of chemical rescue of the adenylyl-Fhit intermediate, **E**-His^{96}-AMP in Equation (3). The pH-dependences in Figs. 2 and 3 constitute documentation that H96G-Fhit binds the monoanionic form of AMP-Im (Scheme 1) as the substrate. At some point in the mechanism, the imidazole ring of AMP-Im must acquire a proton to depart as imidazole. This appears to be a function of His98 in the action of wild-type Fhit on AMP-Im (Figure 8), and His98 may well serve as the proton donor in the hydrolysis of AMP-Im by H96G-Fhit. However, this is not established by the present data, and the mechanism of proton transfer to AMP-Im remains unknown. Comparison of the results for AMP-Im and AMP-*N*-MeIm confirm that the two react by mechanisms that differ in their requirements for proton transfer.

Diffusion Limitations in the Action of Fhit

The data in Figure 6 show that the action of wild-type Fhit is diffusion-limited, but Table 1 shows that the apparent second-order rate constant for the hydrolysis of Ap_3A by Fhit (k_{cat}/K_m) is only 1.2×10^6 M^{-1} s^{-1}. Typical values of rate constants for substrates binding to enzymes are 10^8 M^{-1} s^{-1}, about two orders of magnitude higher than for the diffusion-limited enzymatic hydrolyses catalyzed by Fhit. This paradox can be explained in several ways. Calculations of values of k_{cat}/K_m depend on knowledge of the exact molar concentration of the enzyme under investigation, and they are burdened by the assumption that every enzyme molecule displays exactly the same activity. But an assumption of homogeneity in the structure and activity of enzyme molecules in solution is invalid. In an enzyme with catalytically functional acid (AH) and base (B) groups, the groups may exist mainly as AH and B, but the groups will be in a micro-equilibrium that includes the species A^- and BH^+ resulting from proton transfer. When the latter is the active form, the fraction of active enzyme molecules can be quite small, 1% or less. This is known as reverse protonation and is well-precedented.[36] Reverse protonation of catalytic groups in Fhit is a likely explanation for the paradoxically low value of k_{cat}/K_m.

Experimental Section

Materials: Imidazole and $MgCl_2$ were purchased from Aldrich. AMP, ADP, ATP, potassium phosphoenolpyruvate, Ap_3A, reduced β-nicotinamide adenine dinuceotide (NADH), myokinase, pyruvate kinase, and lactic dehydrogenase were purchased from Sigma. Acetone, methanol, KCl, NaCl, *N*-(2-hydroxyethyl)piperazine-*N*′-2-ethanesulfonic acid (HEPES), 3-(morpholino)propanesulfonic acid (MOPS), 2-(cyclohexylamino)ethanesulfonic acid (CHES), NaOH, and HCl were obtained from Fisher Scientific. Ready gel and gelcode blue stain reagent were from BioRad and Pierce, respectively. AMP-Im and AMP-*N*-MeIm were synthesized as described.[29] Human Fhit and the mutated variants were isolated and purified from *E. coli* strain SG100 sells transformed from pSGA02 carrying the wild-type or mutated gene according to the published method.[29,31]

Assays of Fhit: The coupled assay monitoring AMP formation spectrophotometrically at 340 nm was employed.[29] The coupling enzymes were myokinase (adenylate kinase), pyruvate kinase, and lactate dehydrogenase. Initial rates were measured in a Cary 50 spectrophotometer equipped with a thermostatted cuvette holder. The rates observed as decreasing A_{340} due to consumption of NADH were twice the rate of AMP-Im hydrolysis and, when used to assay the wild-type enzyme, three times the rate of Ap_3A hydrolysis. The detailed procedure was as follows: The assay was carried out at 26.5 °C in 1.00 mL solutions containing 0.1 M MOPS or CHES or 0.55 M imidazole-HCl buffer, as well as 300 μM NADH, 300 μM phosphoenolpyruvate, 100 μM ATP, 75 mM KCl, 2 mM $MgCl_2$, and10–40 units of each coupling enzyme at various pHs. Care was taken to ensure that the coupling enzymes did not limit the rate. The buffer, coupling enzymes, and substrates for the coupling enzymes were separately incubated in the cell holder at 26.5 °C for 20 min and then mixed just before adding either a substrate (AMP-Im, AMP-*N*-MeIm, or Ap_3A) or Fhit. The A_{340} was monitored for 2 min to obtain the background rate (if any) and allow

the temperature to stabilize at 26.5 °C, then the Fhit was added to initiate the enzymatic reaction. The initial rate of decreasing A_{340} (NADH) was measured. The rates were calculated by use of ε_{340} = 6220 $M^{-1}\cdot cm^{-1}$ for NADH. The subunit concentration of Fhit was determined by use of ε_{280} = 8310 $M^{-1}\cdot cm^{-1}$ calculated from the amino acid sequence of Fhit evaluated by the published method.[32]

pH-Rate Profiles: The assay procedure was adapted for use from pH 5.5 to pH 9.0, where the coupling enzymes displayed sufficient activities, and initial rates were measured in triplicate. The good buffers HEPES, MOPS and CHES were employed to cover the pH-range. The data at each pH were fitted to the Michaelis–Menten equation using KaleidaGraph to evaluate V_{max} (k_{cat}) and K_m at that pH. This was repeated at each pH. The non-enzymatic rates for AMP-*N*-MeIm as the substrate were significant and had to be subtracted from the measured initial rates after adding the enzyme. Data were collected at 0.25 or 0.5 pH intervals, and the data were replicated with both buffers at pHs corresponding to buffer changes to ensure the absence of buffer effects. The profiles of log k_{cat} and log k_{cat}/K_m vs. pH were plotted and the data computer fitted to Equation (5), Equation (6), Equation (7), or Equation (8) using the programs HABELL, HBBELL, BELL or BEL2H, respectively, of Cleland.[33]

$$\log y = \log \frac{c}{1 + [H^+]/K_a} \quad (5)$$

$$\log y = \log \frac{c}{1 + K_b/[H^+]} \quad (6)$$

$$\log y = \log \frac{c}{1 + [H^+]/K_a + K_b/[H^+]} \quad (7)$$

$$\log y = \log \frac{c}{1 + [H^+]/K_a + K_b/[H^+] + K_o/[H^+]^2} \quad (8)$$

In fitting the data, y values were the experimental pH-dependent values of k_{cat}^{app} or k_{cat}/K_{mt}^{app}, c was the pH-independent value arising from the fitting procedure, and K_a and K_b were the fitted values of acid dissociation constants.

The Effects of Viscosity on Kinetic Parameters: The kinetic parameters of both wild type and mutated Fhit with different substrates were measured at varying relative viscosity ($\eta_{rel} = \eta/\eta_0$) in 100 mM MOPS buffer containing sucrose at 26.5 °C. Approximate values of relative viscosity of the sucrose used in this study are the following:[34] 0% sucrose, η_{rel} = 0, 14% sucrose, η_{rel} = 1.47, 24% sucrose, η_{rel} = 2.16, 32% sucrose, η_{rel} = 3.15. A plot of k_a/k_a^0 ($k_a = k_{cat}/K_m$, $k_a^0 = k_a$ as $\eta_{rel} = 1$) vs. relative viscosity (η_{rel}) was obtained.

Ionization of AMP-Im: A 40 mM AMP-Im solution in D_2O was adjusted to the desired pD by addition of DCl, and the chemical shifts of C2(H) in the imidazole ring of AMP-Im were measured at pHs from 4.5 to pH 7.5 at 22 °C in a Bruker 200 MHz NMR spectrometer. The chemical shift-values were plotted against pH and fitted to Equation (9) using the TITR program of Cleland. The value of pK_a obtained for the ionization of AMP-Im according to Scheme 1 was 5.6 ± 0.1.

$$Y = A + B/(1 + [H^+]/K) \quad (9)$$

Acknowledgment

This research was supported by Grant No. GM 30480 from the National Institute of General Medical Sciences, U. S. Public Health Service.

[1] M. Ohta, H. Inoue, M. G. Cotticelli, K. Kastury, R. Baffa, J. Palazzo, Z. Siprashvili, M. Mori, P. McCue, T. Druck, C. M. Croce, K. Huebner, *Cell* **1996**, *84*, 587–597.
[2] K. Huebner, P. Hadaczek, Z. Siprashvili, T. Druck, C. M. Croce, *Biochim. Biophys. Acta* **1997**, *1332*, M65–M70.
[3] K. Huebner, P. N. Garrison, L. D. Barnes, C. M. Croce, *Ann. Rev. Genet.* **1998**, *32*, 7–31.
[4] L. Ji, B. Fang, N. Yen, K. Fong, J. D. Minna, J. A. Roth, *Cancer Res.* **1999**, *59*, 3333–3339.
[5] L. Y. Fong, V. Fidanza, N. Zanesi, L. F. Lock, L. D. Siracusa, R. Mancini, Z. Siprashvili, M. Ottey, S. E. Martin, T. Druck, P. A. McCue, C. M. Croce, K. Huebner, *Proc. Natl. Acad. Sci. USA* **2000**, *97*, 4742–4747.
[6] K. R. Dumon, H. Ishii, L. Y. Fong, N. Zanesi, V. Fidanza, R. Mancini, A. Vecchione, R. Baffa, F. Trapasso, M. J. During, K. Huebner, C. N. Croce, *Proc. Natl. Acad. Sci. USA* **2001**, *98*, 3346–3351.
[7] H. Ishii, N. Zanesi, A. Vecchione, F. Trapasso, S. Yendamuri, M. Sarti, R. Baffa, M. J. During, K. Huebner, L. Y. Fong, C. M. Croce, *FASEB J.* **2003**, *17*, 1768–1770.
[8] C. Brenner, P. N. Garrison, J. Gilmour, D. Peisach, D. Ringe, G. A. Petsko, J. M. Lowenstein, *Nature Struct. Biol.* **1997**, *4*, 231–238.
[9] J. E. Wedekind, P. A. Frey, I. Rayment, *Biochemistry* **1995**, *34*, 11049–11061.
[10] C. D. Lima, M. G. Klein, L. B. Weinstein, W. A. Hendrickson, *Proc. Natl. Acad. Sci. USA* **1996**, *93*, 5357–5362.
[11] L. Holm, C. Sander, *Trends Biochem. Sci.* **1997**, *22*, 116–117.
[12] C. D. Lima, K. L. D'Amico, I. Naday, G. Rosenbaum, E. M. Westbrook, W. A. Hendrickson, *Structure* **1997**, *5*, 763–774.
[13] M. Ohta, H. Inoue, M. G. Cotticelli, K. Kastury, R. Baffa, J. Palazzo, Z. Siprashvili, H. C. Pace, P. N. Garrison, A. K. Robinson, L. D. Barnes, A. Draganescu, A. Rösler, G. M. Blackburn, Z. Siprashvili, C. M. Croce, K. Huebner, C. Brenner, *Proc. Natl. Acad. Sci. USA* **1998**, *95*, 5484–5489.
[14] T. L. Field, W. S. Reznikoff, P. A. Frey, *Biochemistry* **1989**, *28*, 2094–2099.
[15] L. J. Wong, P. A. Frey, *J. Biol. Chem.* **1974**, *249*, 2322–2324.
[16] L. J. Wong, P. A. Frey, *Biochemistry* **1974**, *13*, 3889–3894.
[17] L. J. Wong, K. F. Sheu, S. L. Lee, P. A. Frey, *Biochemistry* **1977**, *16*, 1010–1016.
[18] S. L. Yang, P. A. Frey, *Biochemistry* **1979**, *18*, 2980–2984.
[19] K. F. Sheu, J. P. Richard, P. A. Frey, *Biochemistry* **1979**, *18*, 5548–5556.
[20] A. Arabshahi, R. S. Brody, A. Smallwood, T. C. Tsai, P. A. Frey, *Biochemistry* **1986**, *25*, 5583–5589.
[21] J. Kim, F. Ruzicka, P. A. Frey, *Biochemistry* **1990**, *29*, 10590–10593.
[22] T. L. Field, W. S. Reznikoff, P. A. Frey, *Biochemistry* **1989**, *28*, 2094–2099.
[23] S. Geeganage, P. A. Frey, *Methods Enzymol.* **2002**, *354*, 134–148.
[24] J. E. Wedekind, P. A. Frey, I. Rayment, *Biochemistry* **1996**, *35*, 11560–11569.
[25] Y. Huang, P. N. Garrison, L. D. Barnes, *Biochem. J.* **1995**, *312*, 925–932.
[26] L. D. Barnes, P. N. Garrison, Z. Siprashvili, A. Guranowski, A. K. Robinson, S. W. Ingram, C. M. Croce, M. Ohta, K. Huebner, *Biochemistry* **1996**, *35*, 11529–11535.
[27] C. D. Lima, M. D. Klein, W. A. Hendrickson, *Science* **1997**, *278*, 286–290.

[28] A. Abend, P. N. Garrison, W. D. Barnes, P. A. Frey, *Biochemistry* **1999**, *38*, 3668–3676.
[29] K. Huang, A. Arabshahi, Y. Wei, P. A. Frey, *Biochemistry* **2004**, *43*, 7637.
[30] F. J. Ruzika, P. A. Frey, *Bioorg. Chem.* **1993**, *21*, 238–248.
[31] C. Brenner, H. C. Pace, P. N. Garrison, A. K. Robinson, A. Rosler, X. H. Liu, G. M. Blackburn, C. M. Croce, K. Huebner, L. D. Barnes, *Protein Eng.* **1997**, *10*, 1461–1463.
[32] S. C. Gill, P. H. von Hippel, *Anal. Biochem.* **1989**, *182*, 319–326.
[33] W. W. Cleland, *Methods Enzymol.* **1979**, *63*, 103–138.
[34] A. C. Brouwer, J. F. Kirsch, *Biochemistry* **1982**, *21*, 1302–1307.
[35] C. Brenner, *Biochemistry* **2002**, *41*, 9003–9014.
[36] P. A. Sims, T. M. Larsen, R. R. Poyner, W. W. Cleland, G. H. Reed, *Biochemistry* **2003**, *42*, 8298–8306.

Received: July 6, 2005
Published Online: October 10, 2005

